

# Interlayer Energy Transport in Langmuir-Blodgett Polymer Films of Poly[2-(9-carbazolyl)ethyl methacrylate-co-isobutyl methacrylate]

Shinzaburo Ito, Satoru Ohmori, and Masahide Yamamoto\*

Department of Polymer Chemistry, Faculty of Engineering, Kyoto University, Sakyo-ku, Kyoto 606, Japan

Received October 29, 1990; Revised Manuscript Received August 22, 1991

**ABSTRACT:** Excitation energy transport through an ultrathin film has been investigated with a designed structure of copolymers containing carbazole and anthracene chromophores. Poly(isobutyl methacrylate) gives a stable monolayer at the air-water interface, and it is transferrable to a solid substrate. Various kinds of chromophores can be incorporated into this monolayer in the form of methacrylate esters. Using the Langmuir-Blodgett (LB) technique with these copolymers, artificial arrangements of the chromophoric units can be realized in a layered structure of the LB film. The carbazole chromophore exhibited simple monomer emission, and no excimer was detected. This spectroscopic property enabled us to carry out quantitative analyses of the interlayer energy-transfer process. Time-resolved fluorescence spectroscopy clearly showed efficient energy migration among carbazole chromophores. After several steps of interlayer migration, the excitation energy transfers to the anthracene layer coated on the carbazole layers. Although some unknown traps exist in this LB film, statistically random distribution of both the donor and acceptor moieties in each layer results in a high quenching yield of the carbazole excitons. Besides the uniform distribution, an advantage of polymer LB films is the thinness of each layer. These properties make possible the efficient energy transport through the layered structure.

## Introduction

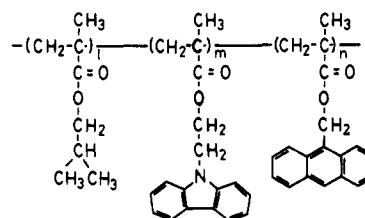
Photophysical processes in polymer matrices have been widely investigated.<sup>1</sup> Excitation energy transfer and migration are fundamental processes caused by interaction between two chromophores in the concentrated system. Artificial control of these photoprocesses is a fascinating subject for many researchers. The Langmuir-Blodgett (LB) technique is an elegant procedure for making an ultrathin film with a thickness of only a few nanometers.<sup>2</sup> LB films are constructed from a monolayer at the air-water interface, and the repeated deposition of the monolayer on a substrate enables one to make spatial arrangements of each layer, e.g., the thickness, sequence, and distance of the photofunctional layers.<sup>3</sup> The designed structure in molecular dimensions results in the control of the photophysically fundamental processes occurring at a distance of a few nanometers.

Recently, some preformed polymers have been found to form a stable monolayer and are transferrable to solid substrates.<sup>4-12</sup> Polymeric materials have a variety of molecular structures which are easily modified with conventional chemical reactions. Various chromophoric units can be introduced with covalent bonds.<sup>13</sup> Such new LB polymers have some remarkable properties: mechanical stability, amorphous character, fewer pinholes, and thinness of each layer.<sup>4c</sup> These characteristics will aid in overcoming the disadvantages of conventional LB materials with long-chain fatty acids.

From the standpoint of polymer photophysics, energy transport from a light-excited chromophore plays an important role in subsequent reactions. In solid matrices, molecular diffusion is negligibly slow, while excitation energy transport due to the multistep migration results in effective sensitization of the reaction sites with a high quantum efficiency. The photophysics of the carbazole chromophore has been widely studied because of the peculiar properties, e.g., two kinds of excimer formation,<sup>14,15</sup> electron transfer, and carrier generation at extrinsic acceptor sites.<sup>16</sup> These processes in the film are highly enhanced by energy transport despite the low

concentration of the reaction sites. In a previous paper, we reported efficient energy migration in a polymer, poly[2-(9-carbazolyl)ethyl methacrylate] (PCzEMA), and the copolymers with methyl methacrylate.<sup>17</sup> These polymers do not form excimers even in the neat film and exhibit only monomer emission. The trap-free character is responsible for efficient energy migration. Because of the spectroscopically pure excited state, the quenching process of the mobile exciton could be quantitatively analyzed by a time-resolved measurement.<sup>18</sup>

In the current study, CzEMA was copolymerized with isobutyl methacrylate. Naito et al. reported that poly(isobutyl methacrylate) yields a stable monolayer.<sup>11</sup> We utilized this polymer as a base unit of the LB film and incorporated a CzEMA unit into this by random copolymerization. As an energy acceptor, a methacrylate monomer having an anthracene unit was also prepared. Using the LB method, some artificial arrangements of the donor and acceptor layers were realized on a quartz plate. Energy migration and transfer processes through the layered structure were investigated. The present work is an approach for controlling fundamental photophysical processes by a designed polymer structure.



## Experimental Section

**Materials.** 2-(9-Carbazolyl)ethyl Methacrylate (CzEMA). A DMF solution of carbazole (19 g; synthesized in this laboratory) and ethylene carbonate (11 g; Wako Pure Chemical Industries, Ltd.) was refluxed for 4 h in the presence of a small amount of sodium hydroxide. After being cooled to room temperature, the mixture was extracted with benzene. Three recrystallizations from hexane gave white crystalline 9-(2-hy-

Table I  
Composition, Molecular Weight, and Refractive Indices of  
Synthesized Isobutyl Methacrylate Copolymers

| sample | content, <sup>a</sup> mol % |       | $M_w,^c \times 10^4$ | $n^d$ |
|--------|-----------------------------|-------|----------------------|-------|
|        | CzEMA                       | AnMMA |                      |       |
| C1     | 1.0                         | 0.0   | 9.8                  | 1.48  |
| C2     | 4.9 (4.4) <sup>b</sup>      | 0.0   |                      | 1.49  |
| C3     | 9.5 (10.0) <sup>b</sup>     | 0.0   | 9.8                  | 1.50  |
| C4     | 15.2 (14.6) <sup>b</sup>    | 0.0   |                      | 1.51  |
| C5     | 20.2 (20.0) <sup>b</sup>    | 0.0   | 12.0                 | 1.52  |
| AC1    | 15.2                        | 0.07  |                      | 1.51  |
| AC2    | 15.2                        | 0.12  | 8.0                  | 1.51  |
| AC3    | 15.0                        | 0.18  |                      | 1.51  |
| AC4    | 15.2                        | 0.38  | 8.0                  | 1.51  |
| A      | 0.0                         | 9.8   | 6.3                  |       |

<sup>a</sup> Based on the monomer molar contents at the reaction. <sup>b</sup> Obtained by measuring <sup>1</sup>H NMR. <sup>c</sup> Determined by GPC calibrated with polystyrene standards. <sup>d</sup> Calculated from two limiting values of PCzEMA, 1.632, and poly(isobutyl methacrylate), 1.477.<sup>22</sup>

droxyethyl)carbazole, mp 89 °C. To a dichloroethane solution of 9-(2-hydroxyethyl)carbazole (8 g) and pyridine (10 mL) was added methacryloyl chloride (6 g; Tokyo Kasei Kogyo Co. Ltd.) at 0 °C. After the mixture was stirred for 3 h at room temperature, the product was extracted with dichloromethane. Recrystallization from methanol solution gave white crystalline CzEMA: mp 88 °C; <sup>1</sup>H NMR (CDCl<sub>3</sub>) δ 1.80 (s, 3 H, methyl), 4.56 (t, 2 H, methylene), 4.60 (t, 2 H, methylene), 5.45 (m, 1 H, vinyl), 5.95 (s, 1 H, vinyl), 7.1–7.6 (m, 6 H, aromatic), 8.10 (d, 2 H, aromatic); IR (KBr) 3060, 2990, 1720, 1630, 1600, 1450, 1160, 740 cm<sup>-1</sup>.

**9-Anthrylmethyl Methacrylate (AnMMA).** This monomer was prepared by the same method as was CzEMA. The esterification of methacryloyl chloride with 9-anthrylmethanol (Nacalai Tesque, Inc.) gave the crystalline monomer: mp 93 °C; <sup>1</sup>H NMR (CDCl<sub>3</sub>) δ 1.90 (s, 3 H, methyl), 5.47 (m, 1 H, vinyl), 6.04 (s, 1 H, vinyl), 6.19 (s, 2 H, methylene), 7.4–8.5 (m, 9 H, aromatic); IR (KBr) 3060, 1710, 1630, 1320, 1160, 900, 740 cm<sup>-1</sup>.

**Isobutyl Methacrylate.** Commercial isobutyl methacrylate (Nacalai Tesque) was purified by distillation under reduced pressure before use.

**Copolymers.** Weighed quantities of these monomers were dissolved in distilled benzene containing azobisisobutyronitrile as an initiator and polymerized at 60 °C. The copolymers obtained were purified by repeated reprecipitation and dried in vacuo. The contents and characteristics of these copolymers are listed in Table I. The contents of monomer units are based on the monomer molar contents in the reaction. These values agree with those of polymer compositions which were obtained from the measurements of <sup>1</sup>H NMR. Three kinds of isobutyl methacrylate copolymers were prepared: (1) a series of copolymers containing various contents of CzEMA, (2) a series of copolymers with a fixed content of CzEMA (ca. 15 mol %) but with small amounts of AnMMA, and (3) a copolymer containing AnMMA (9.8 mol %). They are abbreviated as C<sub>n</sub> (*n* = 1–5), AC<sub>n</sub> (*n* = 1–4), and A, respectively.

**Sample Preparation.** The copolymer was dissolved in benzene (Dojindo Laboratories, spectroscopic grade) and spread onto pure water in a Teflon-coated trough (Kenkosha Model SI-1) with a Wilhelmy-type film balance. The water in the subphase was purified by deionization, distillation, and passage through a water filtration system (Barnstead Nanopure II). The surface film was compressed at a rate of 10 mm min<sup>-1</sup>. A non-fluorescent quartz plate which is a substrate for spectroscopic measurements was cleaned in oxidative sulfuric acid, rinsed repeatedly with pure water, and then dipped in a 10% solution of trimethylchlorosilane in toluene to make it hydrophobic. Instead of the quartz plate, silicon wafers (Shin-etsu Chemical Industries, Ltd.) were used for the measurement of film thickness by ellipsometry. The LB multilayers were prepared by dipping the quartz plate vertically at a speed of 10 mm min<sup>-1</sup>. First, four layers of poly(vinyl octal) (PVO) were deposited on the substrate to remove the effect of the interface and to facilitate the subsequent deposition of chromophoric layers.<sup>7</sup> A good transfer ratio was obtained at a surface pressure of 10 mN m<sup>-1</sup> at 19 °C.

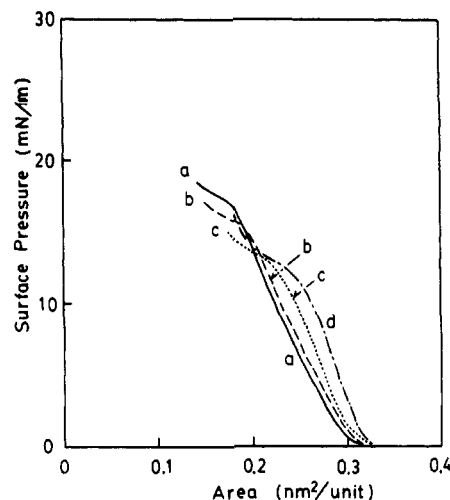


Figure 1. Surface pressure–area isotherms of poly(isobutyl methacrylate) copolymers: (a) C1, (b) C2, (c) C4, and (d) C5.

The transfer of the monolayer took place at each downward and upward dip (Y type). After deposition of the chromophoric layers, four layers of PVO were again deposited to avoid the effect of the air interface. Cast films were prepared from a toluene solution of the copolymer (4 wt %) by a spin-coating method at 5000 rpm for 90 s. The thickness is ca. 400 nm.

**Measurements.** Fluorescence spectra were recorded with a Hitachi 850 fluorescence spectrophotometer. Absorption spectra were measured with a Shimadzu UV-200 spectrophotometer. Fluorescence decay curves were measured by a single photon counting method using a picosecond laser system as the excitation light pulse.<sup>19,20</sup> The details have been described elsewhere.<sup>21</sup> Two types of detectors were used in this study. The fwhm of the instrumental response function was 75 ps for the microchannel plate photomultiplier (Hamamatsu R1564U-01) and 500 ps for the end-on photomultiplier (Hamamatsu R3234). The former was used for measurement of time-resolved fluorescence spectra, and the latter was used for decay curve measurements. Theoretical decay curves were simulated by the Monte Carlo method with a Fujitsu M382 computer. The molecular weights of copolymers were determined by GPC (Tosoh HLC-802UR) on the basis of calibration with polystyrene standards. The thickness of the multilayered films was measured by an ellipsometer (Mizojiri Kogaku).

## Results and Discussion

**Deposition of Polymer LB Films.** A benzene solution of the copolymer (0.01 wt %) was spread at the air–water interface. Figure 1 shows the surface pressure–area isotherms. With increased carbazole content, the collapse pressure becomes low and the limiting area increases from 0.20 to 0.27 nm<sup>2</sup> because of the larger molecular size of the carbazole unit compared to the isobutyl group. In sample C5, which has the highest content of CzEMA (20 mol %), the isotherm shows that the surface film collapses only at 12 mN m<sup>-1</sup>. However, the transfers were all made at 10 mN m<sup>-1</sup> with a transfer ratio of unity within experimental error. Although we prepared another sample containing 30 mol % of CzEMA, it did not form a stable monolayer.

Deposition was successful up to 40 layers. Figure 2A shows the absorbance of multilayered films of C5 vs the number of deposited layers. In this paper, the number of layers represents the one on one side of a substrate. Therefore, the absorbance in Figure 2B corresponds to the value for twice the number of layers on the abscissa, because LB films are transferred to both faces of the quartz plate.

The absorbance for a few number of layers is too small to be measured quantitatively. Therefore, the proportionality was checked from the fluorescence intensity of

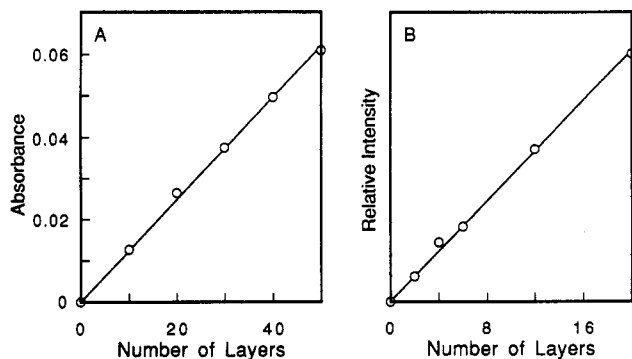


**Figure 2.** Fluorescence intensity and UV absorbance of built-up films as a function of the number of layers (on one side): (A) UV absorbance of C5 films at 296 nm and (B) fluorescence intensity of C1 films at 363 nm.

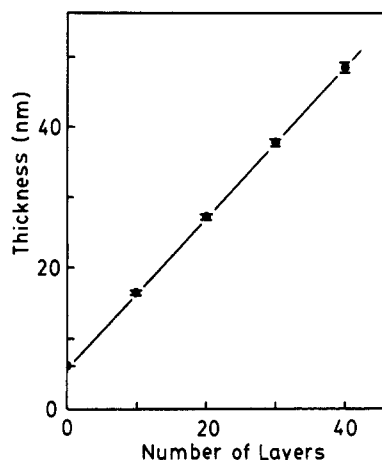


**Figure 3.** Film thickness of the built-up film of C4 as a function of number of layers.

the C1 film. As mentioned later, the fluorescence quantum efficiency of LB films decreases with the number of layers, since some additional quenching process is accelerated by energy migration between the carbazole chromophores as the film thickness increases. However, such a process does not take place at low concentrations of the carbazole unit. Since the content of C1 is only 1 mol %, the fluorescence intensity is proportional to the number of carbazole chromophores per unit area. Figure 2A shows the relation between the fluorescence intensity and the number of layers. The fluorescence intensity is clearly proportional to the number of layers, even in the range of a few layers.

The thickness of LB films was determined by ellipsometry. Figure 3 shows the thickness of C4 films (15.2%) for various numbers of layers. Naito et al. reported the thickness of a poly(isobutyl methacrylate) monolayer to be 1.05 nm.<sup>11</sup> In the present study, the thickness of the chromophoric layers is a critical factor in determining the interlayer photophysical processes. Therefore, we have to obtain the exact value as a fundamental parameter. In Figure 3, the proportionality vs the number of layers is again confirmed up to 40 layers. The intercept at 0 layer shows the sum of the thickness of the oxidized silicon layer at the surface of a wafer and the thickness of the pre-coated PVO layers. These layers have refractive indices quite similar to that of poly(isobutyl methacrylate):  $n_{i-Bu} = 1.477$ .<sup>22</sup> The refractive index of C4 must be known to calculate the precise thickness. The value was estimated to be 1.51 from the content of carbazole units and the refractive index of poly(CzEMA):  $n_{CzEMA} = 1.632$ . The calculation was performed in the range of  $n = 1.48$ –1.52, and the deviation of thickness in the range of  $n$  is

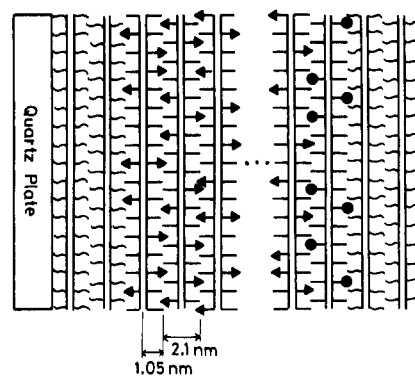


**Figure 4.** Schematic illustration of the multilayer structure of the polymer LB films. Circles represent anthracene chromophores, and triangles are carbazole chromophores.

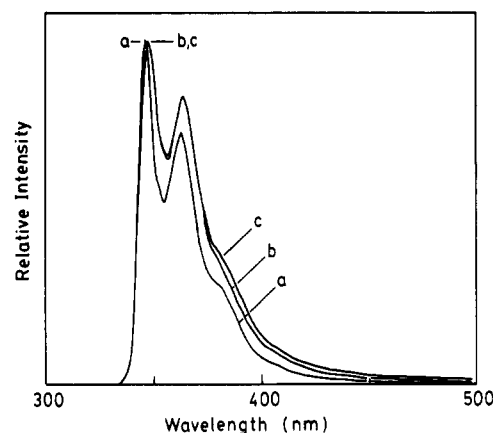


**Figure 5.** Fluorescence spectra of the 20-layer films of (a) C1, (b) C4, and (c) C5. The excitation wavelength is 296 nm. Spectra are recorded with a bandwidth of 2 nm and normalized to the same intensity at the maximum.

represented with error bars in Figure 3. The deviation is negligibly small, and the thickness obtained from the slope is found to be 1.06 nm/layer. This value is in fair agreement with Naito's data for poly(isobutyl methacrylate) homopolymer.<sup>11</sup> This means that the isobutyl parts act as a stable monolayer, and the thickness of LB films is kept constant with the alternation of part of the isobutyl groups with the carbazole units. On the basis of these results, we employed the assumed model shown in Figure 4. Since the film was transferred as a Y-type deposition, the hydrophobic carbazole chromophores are located in two parallel planes with a distance of separation of 2.1 nm. LB films containing carbazole units were piled up to 20 layers, and some of them were coated further with anthracene LB films (A) as energy acceptor layers.

**Fluorescence Characteristics.** Fluorescence spectra of the LB films are shown in Figure 5. All the samples exhibit similar emission spectra consisting of the monomer fluorescence bands of the carbazole chromophore. However, trace amounts of broad emission appeared at longer wavelengths (450–550 nm) as the carbazole concentration increased and the number of layers increased. This additional emission was assigned to exciplex emission of carbazole with unknown acceptors. The acceptors are probably introduced in the LB films during the spreading of the monolayer, since the emission was not seen for the films prepared by spin-coating or casting methods. However, the spectra in Figure 5 show neither partially overlapped excimer nor sandwich excimer emission which would appear at around 380 and 420 nm, respectively.<sup>14,15</sup> As described in the previous paper, P(CzEMA) has no excimer-forming site even in the homopolymer film.<sup>17</sup> The

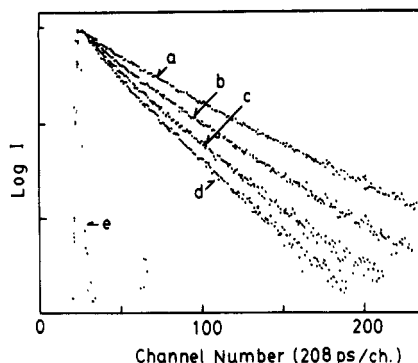


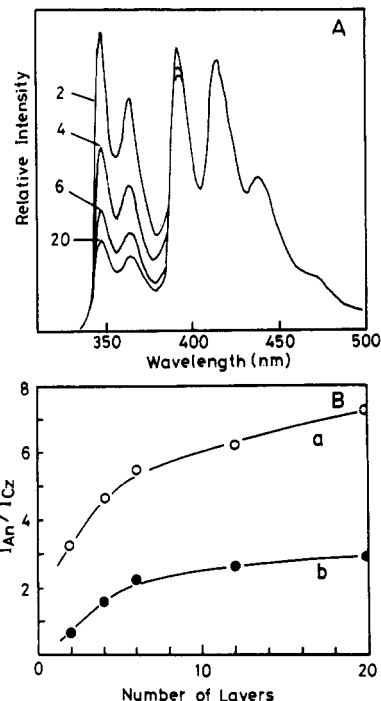
**Figure 6.** Fluorescence decay curves of the carbazole emission in C4 films at various transferred layers: (a) 2-, (b) 6-, (c) 12-, and (d) 20-layer films. Plot e shows the instrument response function for an excitation pulse at 296 nm.

characteristics were retained in the copolymers with isobutyl methacrylate. The combination of two kinds of monomers (isobutyl methacrylate as a base unit to form a stable monolayer and CzEMA as a chromophoric unit) results in a spectroscopically simple excited state of carbazole chromophores in the layered structure of LB films.

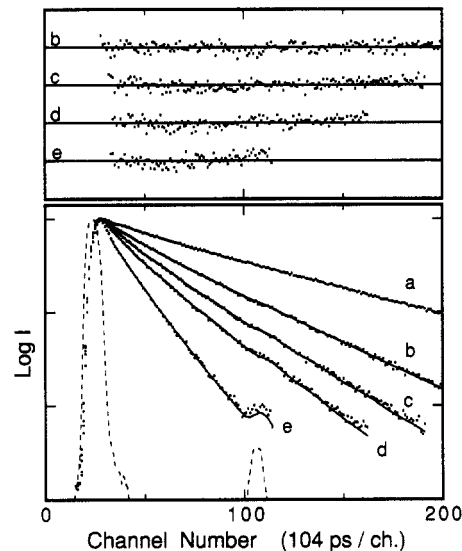
Figure 6 shows fluorescence decay curves of C4 films with various numbers of layers. The shorter decay time for the large number of layers indicates that there are some quenching processes due to unknown impurities. The quenching may be due to energy traps formed by the interaction of the carbazole units. In any case, the quenching processes are accelerated by efficient energy migration among the carbazole chromophores. As reported previously, chromophore concentration is a critical factor in determining the rate of energy migration.<sup>18</sup> In addition to this, the dimensionality must be taken into consideration for the LB system. With an increase in the number of layers, the two-dimensional (2D) system changes to a three-dimensional (3D) system, in which the quenching process takes place with a higher efficiency than that in the 2D system, because of the increase in the number of molecules within the reaction "sphere" of an excited species.

Figure 7A shows the fluorescence spectra of AC2 LB films with various numbers of layers. The intensities are normalized at the second peak of anthracene emission. This indicates that the energy-transfer efficiencies rise with the increase in the film thickness, regardless of constant acceptor concentration. The intensity ratios of anthracene emission to carbazole emission are plotted in Figure 7B. The thickness dependence is an important characteristic of the polymer LB films, resulting from the thinness of each layer. If the thickness is much larger than the reaction radius, photophysical processes in each layer would be independent of the other layers; that is, no thickness dependence would be seen. However, the thickness of polymer LB films is only ca. 1 nm. The distance between the chromophore planes is assumed to be ca. 2 nm (Figure 4), which is comparable to the Förster radius of energy transfer between carbazole groups. Therefore, the incorporated chromophores can easily carry out energy transfer between neighboring layers. Consequently, the interlayer energy migration makes the LB system 3D-like.

**Energy Migration in Cast Films.** The diffusion coefficient of excitation energies in this copolymer was evaluated by decay curve analysis for 3D systems: thick films of AC $n$  ( $n = 1-4$ ), prepared by the spin-coating method. The decay curves are shown in Figure 8. Of course, the decay rate of carbazole emission becomes faster with increased anthracene concentration. However, the



**Figure 7.** (A) Fluorescence spectra of AC2 films at various numbers of transferred layers. Numerals in the figure show the number of layers. The excitation wavelength is 296 nm. (B) Relationship between the number of layers and intensity ratios of anthracene emission ( $I_{An}$  at 416 nm) to carbazole emission ( $I_{Cz}$  at 347 nm): (a) AC4 and (b) AC2.



**Figure 8.** Fluorescence decay curves of C4 and AC $n$  ( $n = 1-4$ ) films prepared by a spin-coating method: (a) C4, (b) AC1, (c) AC2, (d) AC3, and (e) AC4. The solid lines are the curves calculated by the Yokota-Tanimoto model, and the upper part of the figure is the plot of the weight residuals for them. The  $\chi^2$  values are (b) 1.26, (c) 1.46, (d) 1.55, and (e) 1.64. The broken line shows the instrument response function.

decay curves could not be reproduced with the Förster equation based on the static kinetics, in which the excitation energy localizes at the original position of light absorption and directly transfers to an anthracene unit.<sup>23</sup> In these concentrated systems, energy migration exists between carbazole chromophores, which results in efficient diffusion followed by energy transfer to the anthracene moieties. The energy-transfer process involving exciton diffusion can be well represented by the Yokota-Tanimoto Pade model.<sup>24</sup> The equations are given as follows

$$I(t) = I_D(t) \exp(-K[A]) \quad (1)$$

$$K = \frac{4}{3}\pi^{3/2}N'(at)^{1/2}B$$

$$B = [(1 + 10.87x + 15.50x^2)/(1 + 8.743x)]^{3/4}$$

$$a = R_{DA}^6/\tau_D$$

$$x = \Lambda a^{-1/3}t^{2/3}$$

where  $[A]$  is the molar acceptor concentration,  $I(t)$  is the fluorescence decay function of donor emission,  $I_D(t)$  is the fluorescence decay of donor without acceptor,  $N'$  is Avogadro's number per millimole,  $R_{DA}$  is the Förster radius from donor to acceptor,  $\tau_D$  is the lifetime of the donor without any quenching processes, and  $\Lambda$  is the diffusion coefficient of excitation energy.  $R_{DA}$  is evaluated by the spectral overlap between the absorption of the acceptor and the fluorescence of the donor;  $R_{DA} = 2.7$  nm for carbazole-anthracene chromophores. Therefore, only one parameter,  $\Lambda$ , is variable for the curve fitting of  $I(t)$  with the observed decays. The best fit value of  $\Lambda$  is found to be  $9 \times 10^{-6} \text{ cm}^2 \text{ s}^{-1}$ , and the solid lines in Figure 8 show the calculated decay curves. It should be noted that the curves for various acceptor concentrations were calculated with the same value of the diffusion coefficient and fitted well with the experimental data. This result indicates that the energy transport takes place efficiently among carbazole chromophores and that the diffusion length given by  $(6\Lambda t)^{1/2}$  is 8 nm, during the intrinsic lifetime of the carbazole unit, 13 ns. Such an efficient energy transport should occur between neighboring layers of the LB films, although the microstructure is different from the spin-coated films.

**Interlayer Energy Transport in LB Films.** To demonstrate interlayer energy transport through carbazole layers, we prepared some multilayered LB films consisting of  $n$ -layered C4 and then coated these with two layers of A polymer. The samples are abbreviated as  $n\text{C}+2\text{A}$ . The carbazole chromophores were selectively excited at 296 nm with a picosecond laser pulse. At this wavelength, the extinction coefficient of the carbazole unit is 40 times larger than that of the anthracene unit:  $\epsilon_{\text{Cz}} = 12400$  and  $\epsilon_{\text{An}} = 340 \text{ L mol}^{-1} \text{ cm}^{-1}$ . Furthermore, the number of carbazole chromophores per unit area is larger than that of anthracene chromophores. Therefore, the probability of direct excitation of anthracene units is negligibly small compared with the carbazole units. Figure 9 shows the time-resolved fluorescence spectra of 6C+2A and 20C+2A. Each spectrum is normalized to the maximum intensity. For 6C+2A, the excitation energy rapidly transfers to the anthracene unit because of the short mean distance of separation between the donor and acceptor layers. The anthracene emission at around 420 nm appears immediately after the excitation. After 15 ns, all of the energies on the carbazole units have been already quenched and no emission is detected besides the anthracene one. In contrast to this result, Yamazaki et al. reported that fatty acid LB films containing carbazole units showed a slow-decay component in the fluorescence decay curve.<sup>25</sup> Their result indicates that the distribution of chromophores is not statistically random in the LB films and is in an island structure. Such an irregular distribution yields both energy traps and isolated species in the LB plane. The lower quenching yield of the fatty acid system is attributed to this irregular distribution. On the contrary, the quenching of donor emission in the polymer LB film is completed within 15 ns. Recently, we have shown that

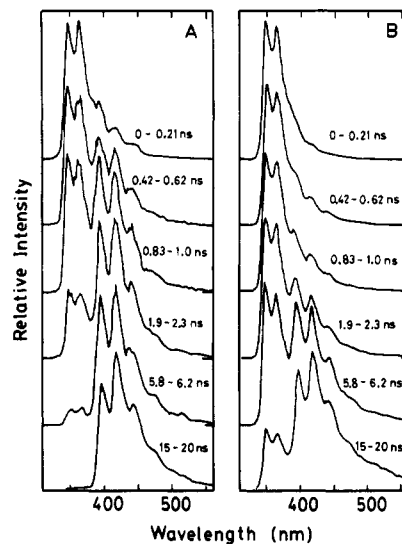


**Figure 9.** Time-resolved fluorescence spectra of (A) 6C+2A and (B) 20C+2A LB films. The excitation wavelength is 296 nm. Time zero corresponds to the time when the excitation laser pulse shows the maximum intensity.

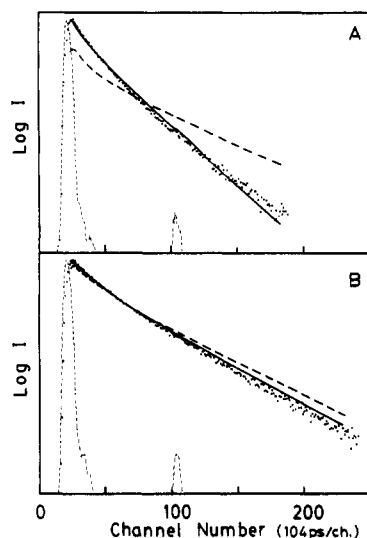


**Figure 10.** Decay curve fitting for (A) 6C+2A and (B) 20C+2A films by the Monte Carlo method involving the energy migration effect. The broken lines show the results for the energy transfer without migration process.

a uniform distribution of chromophores is attainable with polymer LB films containing pyrene chromophore.<sup>13</sup> Therefore, in polymer LB films the excitation energy flows to the acceptor layer smoothly.

The right side of Figure 9 shows the time-resolved spectra of 20C+2A. In this case, the transfer rate is rather slow. The anthracene emission gradually grows, and the carbazole fluorescence is still observed at 15 ns after the pulsed excitation. This means that part of the excited states randomly generated in the carbazole layers cannot reach the active sphere of the anthracene unit. As mentioned above, the thickness of 20-layer films is ca. 20 nm, which is much longer than the diffusion length of energies, 8 nm, measured in the 3D system. Therefore, it is reasonable that the carbazole emission is fully quenched for 6C+2A but only partly for 20C+2A.

**Decay Curve Analysis by the Monte Carlo Method.** Quantitative analysis should be performed on the basis of the fluorescence decay curve. Figure 10 shows the decay curves of carbazole emission at 363 nm. With an increase in the number of layers, the decay rates become slower

because of the increase in the mean distance to the acceptor layers. We tried to simulate these decay curves by calculation with the Monte Carlo method including the energy migration process.<sup>26</sup> The model is based on the following assumptions.

(1) Energy transfer (carbazole–anthracene) and energy migration (carbazole–carbazole) processes occur by dipole–dipole interaction expressed by the Förster formula<sup>23</sup>

$$W_{DA} = (R_{DA}/r_{DA})^6/\tau_D \quad (2)$$

where  $W_{DA}$  is the probability of energy transfer per unit time from an excited donor molecule D to an acceptor molecule A,  $r_{DA}$  is the distance between D and A, and  $R_{DA}$  is the critical transfer radius (Förster radius) at which donor D has an equal probability of energy transfer to other decay processes, and  $\tau_D$  is the unquenched lifetime of D.

(2) The Förster radius is given by the fluorescence spectrum of D and the absorption spectrum of A as follows<sup>23,27</sup>

$$R_{DA} = [(9000 \ln(10K^2\Phi_D))J/(128\pi^5r^4N)]^{1/6} \quad (3)$$

$$J = \int F_D(\lambda) \epsilon_A(\lambda) \lambda^4 d\lambda \quad (4)$$

where  $K^2$  is the orientation factor, in this case, the value is  $2/3$  since depolarization of excited donors occurs by “intralayer” migration before “interlayer” migration,  $n$  is the refractive index of the medium,  $\Phi_D$  is the quantum efficiency of donor D,  $F_D(\lambda)$  is the fluorescence spectrum normalized such that  $\int F_D(\lambda) d\lambda = 1$ , and  $\epsilon_A(\lambda)$  is the extinction coefficient of A at wavelength  $\lambda$ . The calculated values of  $R_{DA}$  are 2.7 nm for carbazole to anthracene units and 1.9 nm for carbazole to carbazole chromophores.

(3) Each chromophore exists in a plane of LB films as shown in Figure 4. The distance of a pair of adjacent layers is 2.1 nm due to the Y-type deposition, but the chromophores are in contact with the next layers. Therefore, the plane density of chromophores is set to be twice the value in a monolayer.

(4) The chromophores are uniformly distributed in the lattice of the plane. The unit size of the lattice was calculated from the plane density of chromophores which is determined by the surface area at the deposition and the concentration of chromophores. The calculated lattice is  $50 \times 50$  units: this size is large enough since the results were not affected even if a  $100 \times 100$  unit area was used.

(5) An excited state was generated at a carbazole layer, and the transfer (migration) probabilities to other layers were calculated. According to the Monte Carlo method, the excitation energy moves to different layers with the calculated transfer probability until it is captured by the anthracene layers. The calculations were repeated for 1000 patterns of random walk. The obtained survival probabilities at time  $t$ , that is, the decay of a carbazole chromophore, were added and normalized.

The solid lines in Figure 10 show the calculated functions. The calculated curves represent well the experimental ones for various numbers of layers where there is no adjustable parameter in this calculation. Strictly speaking, the curve fitting is not as good. The deviation may be due to the simple model of the film structure. The actual decay curves involve the components of fast decay compared to the theoretical one. The fact shows that the layer structure is disordered and the mean distance of the donor and acceptor is shorter than the assumed model. The results, however, clearly show the effect of energy transport through the carbazole layers.

**Table II**  
Calculated Rates of Interlayer Energy Migration and Transfer

| layer, $n$ | $k_{\text{mig}}, \text{s}^{-1}$ | $k_{\text{trans}}, \text{s}^{-1}$ |
|------------|---------------------------------|-----------------------------------|
| 0          | $8.1 \times 10^9$               | $1.8 \times 10^{10}$              |
| 2          | $7.0 \times 10^8$               | $1.3 \times 10^9$                 |
| 4          | $4.4 \times 10^7$               | $8.1 \times 10^7$                 |
| 6          | $8.6 \times 10^6$               | $1.6 \times 10^7$                 |

We also obtained the theoretical curves with the same assumption except that an interlayer migration process does not exist. If the migration process is neglected, the Monte Carlo method is not necessary. The decay function of Cz at each layer was obtained by calculating the direct transfer probability to the anthracene layer. The decay function of a whole LB film was calculated by adding the functions of several layers. The resulting decay curves deviate to a great extent as shown by the broken lines in Figure 10.

Table II shows the calculated rates of energy migration and transfer from a carbazole layer to different layers. The energy-transfer rate between two planes can be directly calculated as the sum of transfer rates from chromophore to other objective chromophores. In this case, we need not use the random process (the Monte Carlo method). The number in the first column means that the objective layer is the  $n$ th layer from the excitation energy: The distance is given by  $1.05n$  nm where  $n = 0$  means intralayer migration or transfer (see Figure 4). The value for intralayer migration is 10 times larger than that for interlayer migration, but the intralayer process is ineffective on energy transport to the acceptor layer. The migration rate to the adjacent layers is still so fast ( $7.0 \times 10^8 \text{ s}^{-1}$ ) that iterative migration occurs considerably during the lifetime.

## Conclusions

Multilayered LB films containing carbazole and anthracene chromophores were prepared from copolymers with isobutyl methacrylate, which is a useful base unit to make the LB film. The thickness of the monolayer is quite thin, ca. 1 nm, which is smaller than the radii of energy transfer between carbazole–carbazole or carbazole–anthracene chromophores. Efficient energy transport through the thin films was demonstrated by time-resolved fluorescence spectroscopy. Numerical simulation of the interlayer migration and transfer processes was carried out with the Monte Carlo method, where the excitation energy migrates according to the rate for the Förster mechanism. The result showed that, after several steps of interlayer migration, the excitation energy transfers to the anthracene layer coated on the outside of carbazole layers. Although some unknown traps exist in this LB film, statistically uniform distribution in the planes of the donor and acceptor chromophores results in a high quenching yield of the carbazole energies. An advantage of the polymer LB film is the uniform distribution of chromophoric units. If there are some defects, aggregation or pinholes with respect to the chromophore density, the energy transfer will be partly restricted by the defect part. Another advantage of polymer LB films is the thinness of each layer. This property is also responsible for the efficient energy transfer between neighboring layers. Thus, the polymer LB film is a promising material for realizing an artificial molecular assembly in which photophysical processes can be controlled.

**Acknowledgment.** We thank Drs. Y. Yonezawa and M. Kawasaki (Department of Industrial Chemistry, Fac-

ulty of Engineering, Kyoto University) for their measurements of ellipsometry. This work was partially supported by a Grant-in-Aid for Scientific Research (No. 01550692) and a Grant-in-Aid for Scientific Research on Priority Areas, New Functionality Materials-Design, Preparation and Control (No. 01604567), from the Ministry of Education, Science and Culture of Japan.

## References and Notes

- (1) (a) Guillet, J. *Polymer Photophysics and Photochemistry*; Cambridge University: Cambridge, 1985. (b) *Polymer Photophysics*; Phillips, D., Ed.; Chapman and Hall: London, 1985. (c) *Photophysical and Photochemical Tools in Polymer Science*; Winnik, M. A., Ed.; NATO ASI Series; Reidel: Dordrecht, 1986. (d) *Photophysics of Polymers*; Hoyle, C. E., Torkelson, J. M., Eds.; ACS Symposium Series 358; American Chemical Society: Washington, DC, 1987.
- (2) (a) Blodgett, K. B. *J. Am. Chem. Soc.* **1935**, *57*, 1007. (b) Blodgett, K. B.; Langmuir, I. *Phys. Rev.* **1937**, *51*, 964.
- (3) Kuhn, H.; Möbius, D.; Bücher, H. In *Physical Methods of Chemistry*; Weissberger, A., Rossiter, B. W., Eds.; Wiley: New York, 1972; Vol. 1, Part 3B, p 557.
- (4) (a) Tredgold, R. H.; Winter, C. S. *J. Phys. D.; Appl. Phys.* **1982**, *15*, L55. (b) Tredgold, R. H.; Winter, C. S. *Thin Solid Films* **1983**, *99*, 81. (c) Tredgold, R. H. *Thin Solid Films* **1987**, *152*, 223.
- (5) Takenaka, T.; Harada, K.; Matsumoto, M. *J. Colloid Interface Sci.* **1980**, *73*, 569.
- (6) (a) Kawaguchi, T.; Nakahara, H.; Fukuda, K. *J. Colloid Interface Sci.* **1985**, *104*, 290. (b) Kawaguchi, T.; Nakahara, H.; Fukuda, K. *Thin Solid Films* **1985**, *133*, 29.
- (7) (a) Oguchi, K.; Yoden, T.; Sanui, K.; Ogata, N. *Polym. J.* **1986**, *18*, 887. (b) Watanabe, M.; Kosaka, Y.; Sanui, K.; Ogata, N.; Oguchi, K.; Yoden, T. *Macromolecules* **1987**, *20*, 452. (c) Watanabe, M.; Kosaka, Y.; Oguchi, K.; Sanui, K.; Ogata, N. *Macromolecules* **1988**, *21*, 2997. (d) Oguchi, K.; Yoden, T.; Kosaka, Y.; Watanabe, M.; Sanui, K.; Ogata, N. *Thin Solid Films* **1988**, *161*, 305.
- (8) Mumby, S. J.; Swalen, J. D.; Rabolt, J. F. *Macromolecules* **1986**, *19*, 1054.
- (9) (a) Laschewsky, A.; Ringsdorf, H.; Schmidt, G.; Schneider, J. *J. Am. Chem. Soc.* **1987**, *109*, 788. (b) Ringsdorf, H.; Schmidt, G.; Schneider, J. *Thin Solid Films* **1987**, *152*, 207.
- (10) Duda, G.; Schouten, A. J.; Arndt, T.; Lieser, G.; Schmidt, G. F.; Bubeck, C.; Wegner, G. *Thin Solid Films* **1988**, *159*, 221.
- (11) Naito, K. *J. Colloid Interface Sci.* **1989**, *131*, 218.
- (12) Matsumoto, M.; Itoh, T.; Miyamoto, T. In *Cellulosics Utilization*; Inagaki, H., Phillips, G. O., Eds.; Elsevier: London, 1989, p 151.
- (13) (a) Ito, S.; Okubo, H.; Ohmori, S.; Yamamoto, M. *Thin Solid Films* **1989**, *179*, 445. (b) Ohmori, S.; Ito, S.; Yamamoto, S.; Yonezawa, Y.; Hada, H. *J. Chem. Soc. Chem. Commun.* **1989**, 1293. (c) Ohmori, S.; Ito, S.; Yamamoto, M. *Macromolecules* **1990**, *23*, 4047.
- (14) Johnson, G. E. *J. Chem. Phys.* **1975**, *62*, 4697.
- (15) Itaya, A.; Okamoto, K.; Kusabayashi, S. *Bull. Chem. Soc. Jpn.* **1976**, *49*, 2082.
- (16) Pfister, G.; Williams, D. J. *J. Chem. Phys.* **1974**, *61*, 2416.
- (17) Ito, S.; Yamashita, K.; Yamamoto, M.; Nishijima, Y. *Chem. Phys. Lett.* **1985**, *117*, 171.
- (18) Ohmori, S.; Ito, S.; Yamamoto, M. *Ber. Bunsenges. Phys. Chem.* **1989**, *93*, 815.
- (19) O'Connor, D. P.; Phillips, D. *Time-Correlated Single Photon Counting*; Academic: London, 1984.
- (20) Yamazaki, I.; Tamai, N.; Kume, H.; Tsuchiya, H.; Oba, K. *Rev. Sci. Instrum.* **1985**, *56*, 1187.
- (21) (a) Ito, S.; Takami, K.; Yamamoto, M. *Makromol. Chem., Rapid Commun.* **1989**, *10*, 79. (b) Ito, S.; Takami, K.; Tsujii, Y.; Yamamoto, M. *Macromolecules* **1990**, *23*, 2666.
- (22) *Polymer Handbook*; Brandrup, J., Immergut, E. H., Eds.; Wiley: New York, 1975.
- (23) Förster, T. *Z. Naturforsch.* **1949**, *4a*, 321.
- (24) Yokota, M.; Tanimoto, O. *J. Phys. Soc. Jpn.* **1967**, *22*, 779.
- (25) (a) Tamai, N.; Yamazaki, T.; Yamazaki, I. *J. Phys. Chem.* **1987**, *91*, 841. (b) Yamazaki, I.; Tamai, N.; Yamazaki, T.; Murakami, A.; Mimuro, M.; Fujita, Y. *J. Phys. Chem.* **1988**, *92*, 5035.
- (26) Barner, W. F. *Jour. SIAM.* **1958**, *6*, 438.
- (27) Berlman, I. B. *Energy Transfer Parameters of Aromatic Compounds*; Academic: New York, 1973.

**Registry No.** CzEMA, 15657-91-7; CzEMA/H<sub>2</sub>C=C(Me)C(O)OBu-*i* (copolymer), 137145-30-3; CzEMA/AnMMA/H<sub>2</sub>C=C(Me)C(O)OBu-*i* (copolymer), 137145-31-4; AnMMA/H<sub>2</sub>C=C(Me)C(O)OBu-*i* (copolymer), 137145-32-5; H<sub>2</sub>C=C(Me)COCl, 920-46-7; ethylene carbonate, 96-49-1; carbazole, 86-74-8; 9-(2-hydroxyethyl)carbazole, 1484-14-6.